

Large Signal Simulink Models of a Boost Converter in CCM and DCM modes

Abstract. This paper presents simulation models of an open loop boost converter. The proposed models are applicable to both; continuous conduction mode CCM and discontinuous conduction mode DCM. We derive two variants of the model, applicable for instantaneous and averaged signal analysis. The proposed models are open loop systems, without control feedback, and they are useful for dynamic states simulations and in alternative control closed loop systems investigations. We implemented the models in Matlab/Simulink and compared the simulated waveforms with oscilloscopes recorded from a physical DC/DC system.

Streszczenie. W artykule przedstawiono modele symulacyjne zasilacza dławikowego podwyższającego napięcie wyjściowe dla sygnałów chwilowych i sygnałów uśrednionych. Modele uwzględniają dwa stany pracy zasilacza, ciągły i nieciągły prąd dławika. Modele dotyczą struktury otwartej układu, bez układu sterowania i sprzężeń zwrotnych. Mogą być wykorzystane do badania różnych struktur sterowania zasilacza. Przedstawiono struktury modeli z wykorzystaniem programu Matlab/Simulink oraz porównano przebiegi symulacji z przebiegami w układzie rzeczywistym. (Modele zasilacza dławikowego podwyższającego napięcie dla stanów CCM i DCM)

Keywords: Boost converter model, DC/DC, CCM, DCM

Słowa kluczowe: Model zasilacza dławikowego, ciągły i nieciągły prąd dławika, przekształtnik DC/DC

Introduction

Boost converter is a simple power circuit that has gained much popularity in applications such as: uninterruptible power supply (UPS) units, power factor correction (PFC) rectifiers, or photovoltaic energy conversion systems [6, 9]. The dynamic properties of a boost converter are well known and rely primarily on the inductor current [3, 11, 13]. If the current flowing through the inductor is always nonzero, then the circuit operates in the continuous conduction mode (CCM), otherwise the discontinuous conduction mode (DCM) is attained. In steady state conditions the circuit can easily be analyzed using linear algebra. However, any dynamic changes in the parameters may result in transitions between modes which makes the analysis problem more difficult.

In simulations the mode of operation is very often assumed. For example for most DC/DC converters it is advantageous to operate in the CCM mode and for this reason converter control investigations are conducted as if this was the only mode in which the circuit operated. On the other hand, a boost converter used as an AC/DC converter with PFC is typically operated in the DCM mode or at the mode transition boundary [4, 10]. For these reasons any model should be able to incorporate both modes of operation.

In recent studies emphasis was typically placed on proposing new control algorithms giving few details regarding the boost converter models used. Canalli, Cobos et al. [1] present models and describe the properties of several DC/DC converters, without conducting any experimental validation. Guinjoan [5] presents a control algorithm for an averaged model and compares the obtained waveforms with an exact, instantaneous model. A similar circuit is analyzed in [8] where Matlab/Simulink package is used to perform the analysis of the nonlinear chaotic phenomenon. Average converter models are also presented in [2], however experimental validation is presented only for a buck converter.

In this paper we are presenting two boost converter models that incorporate the transitions between CCM and DCM modes. The proposed models are derived from differential equations describing the circuit and adapted for implementation in numerical simulation software. We implemented the models in Matlab/Simulink and compared the computer generated waveforms with measurements from a physical system. We also demonstrate that under certain conditions the inductor series resistance R_L has very little influence on the CCM/DCM switching boundary.

Circuit modeling

A schematic diagram of a boost converter together with reference voltage orientations and current flows is presented in Fig. 1. To simplify the analysis we assume that all circuit elements are ideal. This means that the transistor and the diode steady state characteristics are identical with the semiaxes of the current-voltage plane and that their switching times are zero. The resistance of the inductor L and both; the equivalent series resistance ESR and the equivalent series inductance ESL of the capacitor C are neglected. Furthermore, it is assumed that the transistor is being switched with a constant frequency f and that the control signal has a duty cycle d .

Instantaneous simulation model

Consider a situation in which at $t = 0$ the transistor is turned on and remains on for the duration t_{on} . Then for $0 \leq t \leq t_{on}$ the diode is reverse biased and the inductor current and capacitor voltage are given by

$$(1) \quad L \frac{di_L(t)}{dt} = V_s,$$

$$(2) \quad C \frac{dv_C(t)}{dt} = -\frac{1}{R} v_C(t),$$

with some initial conditions $i_L(0) \geq 0$ and $v_C(0) \geq 0$. Observe that when the transistor is on, the input energy is stored in the inductance and the energy from the capacitor is transferred to the load resistance R .

When the transistor is turned off after a delay t_{on} the circuit configuration changes. To simplify notation let us introduce a new time coordinate τ aligned to the time instance when the transistor switching occurs, i.e. $\tau = t - t_{on}$. Depending on the diode state, for $0 \leq \tau \leq \tau_{off}$, the circuit is described by different sets of equations. If the diode D is on, then $i_L(\tau) > 0$ for all τ and

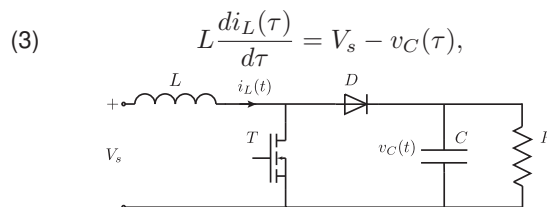


Fig. 1. DC-DC boost converter schematic diagram.

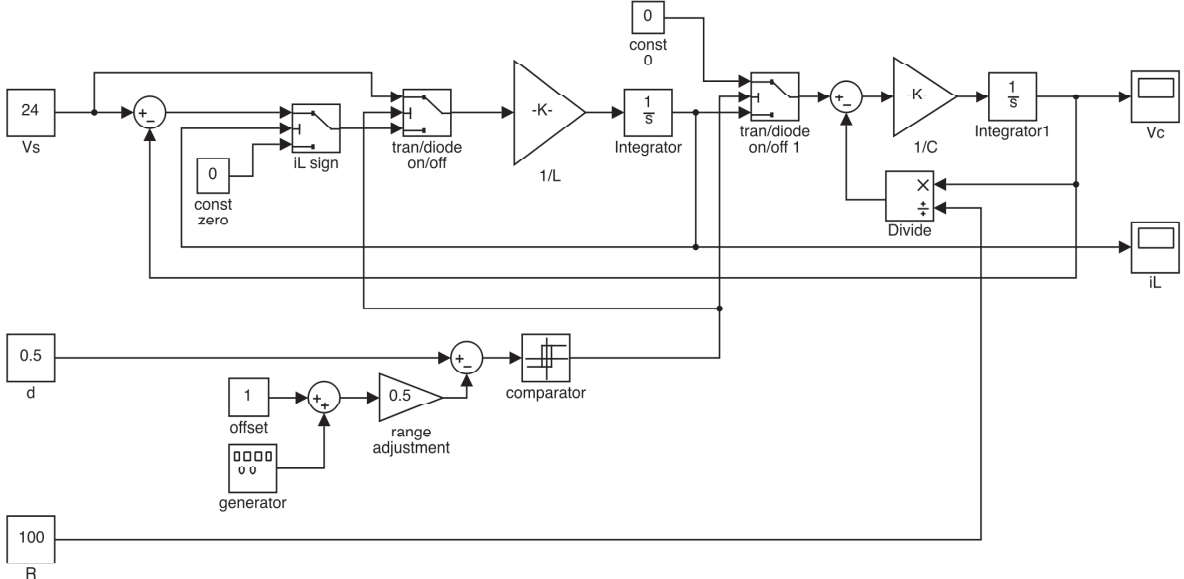


Fig. 2. A Matlab/Simulink block diagram of a circuit realizing the proposed instantaneous DC/DC boost converter model.

$$(4) \quad C \frac{dv_C(\tau)}{d\tau} = i_L(\tau) - \frac{1}{R} v_C(\tau),$$

with initial conditions $i_L(0) > 0$ and $v_C(0) > 0$ respectively. The condition that the inductor current is strictly positive for all τ implies that this current flows without interruption and hence such a state is called the *continuous current mode* or CCM for short. On the other hand, if the diode D is off, the current $i_L(\tau) = 0$ starting at some time instance τ' and remains zero throughout the remainder of the cycle, then the circuit is described by

$$(5) \quad L \frac{di_L(\tau)}{d\tau} = 0, \quad i_L(\tau) = 0,$$

$$(6) \quad C \frac{dv_C(\tau)}{d\tau} = -\frac{1}{R} v_C(\tau),$$

with an initial condition $v_C(\tau') > 0$. In this case the current flow is interrupted and hence the name *discontinuous current mode* or DCM given to the converter operating under such conditions.

With the ideal diode assumption in place, the condition $i_L(\tau) \geq 0$ always holds. When the transistor is off the diode state is determined by the inductor current value. If $i_L(\tau) > 0$ the diode is on, and it is off when $i_L(\tau) = 0$. However, when conducting numerical simulations the inductor current is calculated by integration, and therefore it never achieves zero exactly. This suggests that in a calculation step the case $i_L(\tau) \leq 0$ is possible because $V_s < v_C$. This means that the simulation model given by (5) and (6) describing the diode in the non-conducting state, when $i_L(\tau) \leq 0$, should be modified as

$$(7) \quad L \frac{di_L(\tau)}{d\tau} = 0, \quad i_L(\tau) = \epsilon,$$

$$(8) \quad C \frac{dv_C(\tau)}{d\tau} = \epsilon - \frac{1}{R} v_C(\tau),$$

where ϵ is a small negative quantity. The numerical value of ϵ is computed in the previous calculation step, when the diode D was conducting. Such a formulation can be motivated by the physics of semiconductor devices. Physical diodes under reverse bias do conduct very small current through the

junction. If the discretization time step is sufficiently small the parameter ϵ has no influence on the behavior of the converter.

A Matlab/Simulink implementation of this model is presented in Fig. 2. This block diagram implements the system described by equations (1) – (4) and (7), (8).

Averaged simulation model

This model can be used to analyze dynamic properties of a converter for current and voltage averages computed during a single work period T . In a quasi-steady state average values remain constant, they do change however during dynamic transitions. The dynamic properties of the converter in the CCM mode are derived under the assumption that the inductor current and the capacitor voltage remain constant during a single period, and that they vary between periods. Let $\langle x(t) \rangle$ denote an average of the quantity $x(t)$ computed over the period T , then the circuit in the CCM mode can be described by

$$(9) \quad L \frac{d \langle i_L(t) \rangle}{dt} = V_s - (1-d) \langle v_C(t) \rangle$$

$$(10) \quad C \frac{d \langle v_C(t) \rangle}{dt} = (1-d) \langle i_L(t) \rangle - \frac{1}{R} \langle v_C(t) \rangle,$$

with initial conditions $\langle i_L(0) \rangle$ and $\langle v_C(0) \rangle$ [12]. If V_s is the input and v_C the output a linear, second order model is obtained. The system is typically controlled by the duty cycle d and the model is frequently used in analytic methods for converter control. Often, it is assumed that a DC/DC converter operates in the CCM mode just because it is the desired mode of operation having several advantages over DCM.

In order to include the operation mode change it is necessary to consider the averaged model for the DCM case. In deriving the time averaged quantities it is helpful to note that the energy stored in the inductor at the beginning and the end of each modulator cycle T is equal to zero. This in turn allows to derive the average current through the inductor using simple algebra, rather than differential calculus. The average inductor current is given by

$$(11) \quad \langle i_L(t) \rangle = \frac{V_s d^2 T \langle v_C(t) \rangle}{2L (\langle v_C(t) \rangle - V_s)},$$

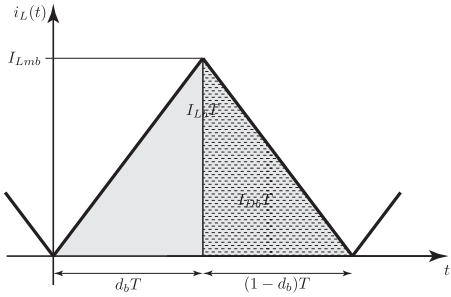


Fig. 3. Inductor current waveform for the CCM/DCM boundary state. The gray area corresponds to $I_{Lb}T$ and the dashed area to $I_{Db}T$.

and the average current through the diode D is

$$(12) \quad \langle i_D(t) \rangle = \frac{V_s^2 d^2 T}{2L(\langle v_C(t) \rangle - V_s)}.$$

The equations (11) and (12) together with the differential equation of an RC circuit

$$(13) \quad C \frac{d\langle v_C(t) \rangle}{dt} = \langle i_D(t) \rangle - \frac{1}{R} \langle v_C(t) \rangle$$

fully describe the converter in the DCM mode. Having the duty cycle d as the input and v_C as the output a first order non-linear model is obtained [7]. Instantaneous changes of the average inductor current are possible, and the average voltage across the capacitor C can be derived using the properties of an RC circuit.

In order to obtain an averaged model for both, CCM and DCM modes, let us consider the conditions that have to hold in both cases. These conditions can be derived by analyzing the inductor current at the conductance boundary, a time evolution plot of this current is illustrated in Fig. 3. Assuming that v_C remains constant during a single period T , and as long as the transistor remains on, the inductor current increases until it reaches a maximum I_{Lmb} at time instance $d_b T$. When the transistor is switched off, the inductor current, at that point equal to the diode current, decreases to zero in $(1 - d_b)T$. These considerations are valid as long as $v_C > V_s$. If this condition does not hold, the converter is in the CCM regime. It follows that the boundary duty cycle d_b is given by

$$(14) \quad d_b = \frac{\langle v_C(t) \rangle - V_s}{\langle v_C(t) \rangle},$$

and the maximal inductor current value is

$$(15) \quad I_{Lmb} = \frac{V_s (\langle v_C(t) \rangle - V_s) T}{L \langle v_C(t) \rangle}.$$

At the conduction boundary the average diode current, equal to the load current, is

$$(16) \quad I_{Db} = \frac{V_s^2 (\langle v_C(t) \rangle - V_s) T}{2L \langle v_C(t) \rangle^2},$$

and the inductor current is

$$(17) \quad I_{Lb} = \frac{V_s (\langle v_C(t) \rangle - V_s) T}{2L \langle v_C(t) \rangle}.$$

As long as the average inductor current $\langle i_L(t) \rangle$ is smaller than the average inductor current at the conductance boundary, i.e. $\langle i_L(t) \rangle < I_{Lb}$ then this current is discontinuous and the converter operates in the DCM mode. On the other hand if $\langle i_L(t) \rangle > I_{Lb}$ the system is in the CCM mode.

It is further required to analyze the case when the capacitor voltage v_C , equal to the output voltage, is smaller than

Table 1. Test circuit parameters.

Parameter	Value
Frequency, f	45.78 kHz
Supply voltage, V_s	24V
Duty cycle, d	0.5
Inductance, L	230 μ H
Inductor resistance, R_L	0.5 Ω
Capacitance, C	47 μ F
Load resistance, R	100 Ω
Transistor	IRF 630
Diode	BYV42/200
Modulator	TDA1060
Controller	TC429

V_s . Such a situation can occur in dynamic states, for example during initial circuit power up. In summary the conditions defining the operation mode are as follows:

- $\langle v_C(t) \rangle \leq V_s$, always CCM mode;
- $\langle v_C(t) \rangle > V_s$ and $\langle i_L(t) \rangle \leq I_{Lb}$, DCM mode;
- $\langle v_C(t) \rangle > V_s$ and $\langle i_L(t) \rangle = I_{Lb}$, conduction boundary;
- $\langle v_C(t) \rangle > V_s$ and $\langle i_L(t) \rangle > I_{Lb}$, CCM mode.

Equations (9) and (10) describing the circuit in the CCM mode, together with (11) through (13) for the circuit in the DCM mode and the switching conditions defined in the previous paragraph are sufficient to implement the averaged converter model.

Figure 4(a) shows a Matlab/Simulink implementation of the averaged simulation model. Switching between the CCM and DCM modes is realized by comparing to the boundary value the average inductor current computed for every cycle T . In order to avoid an arithmetic loop a first order block with a very small time constant was introduced into the model. The submodules modeling the inductor current $\langle i_L(t) \rangle$ in the respective modes are presented in Fig. 4(b) and 4(c).

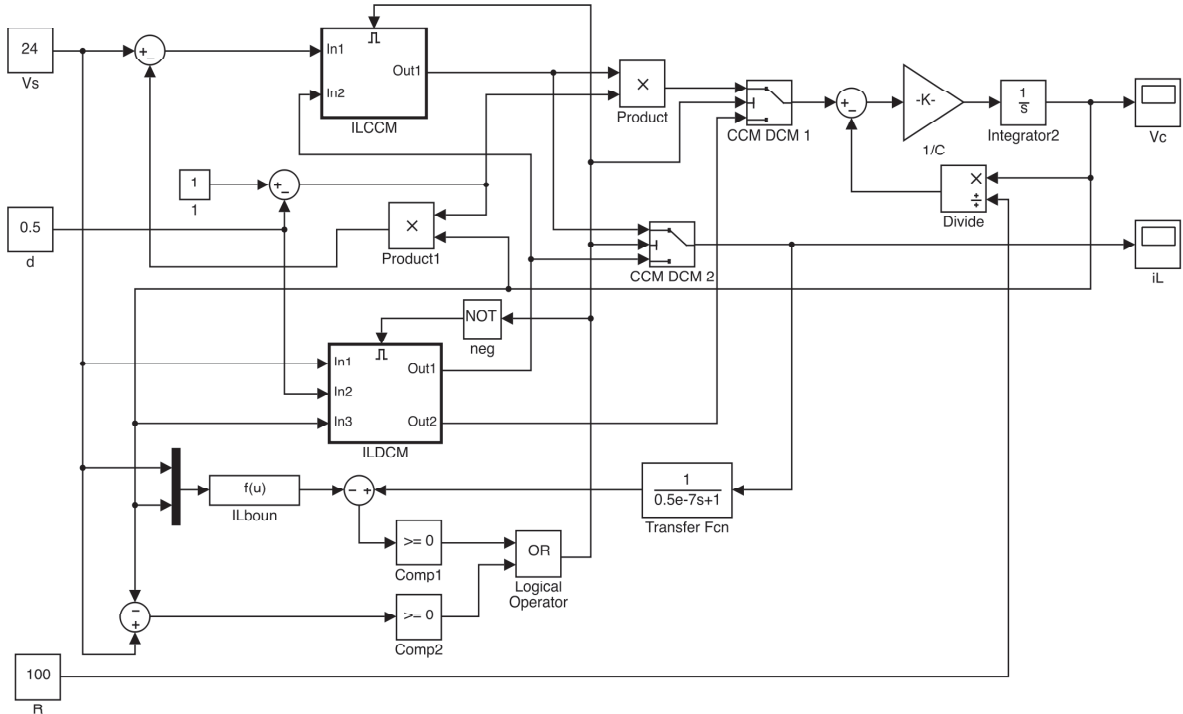
Experimental verification

Both models were experimentally verified by comparing simulation results with waveforms obtained from a real circuit. The circuit was constructed to ascertain test conditions identical to those used in simulations. Table 1 lists basic parameters of the physical circuit. In order to eliminate core saturation for large values of current an air core inductor was used. The modulator circuit was operating in the open loop mode, i.e. both soft start and current control were switched off. Finally, both simulation models were slightly modified to include the inductor resistance R_L as well as the resistance of a current probe connected in series.

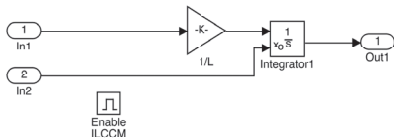
When the inductor resistance R_L is included in the analysis, the inductor current no longer changes linearly, as demonstrated in Fig. 3, but exponentially. This means that equations (14) – (16) which are used to determine the CCM/DCM switching thresholds in the averaged model should incorporate this resistance as well. The modified equations are

$$(18) \quad d_{Rb} = \frac{L}{R_L T} \ln \frac{V_s + (\langle v_C(t) \rangle - V_s) e^{\frac{R_L T}{L}}}{\langle v_C(t) \rangle},$$

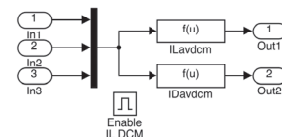
$$(19) \quad I_{LmRb} = \frac{V_s (\langle v_C(t) \rangle - V_s) \left(e^{\frac{R_L T}{L}} - 1 \right)}{R_L \left(V_s + (\langle v_C(t) \rangle - V_s) e^{\frac{R_L T}{L}} \right)},$$



(a) Block diagram



(b) $\langle i_L(t) \rangle$ CCM subblock.



(c) $\langle i_L(t) \rangle$ DCM subblock.

Fig. 4. A Matlab/Simulink block diagram of the averaged DC/DC boost converter model. The inductor current CCM and DCM models are outlined in more detail.

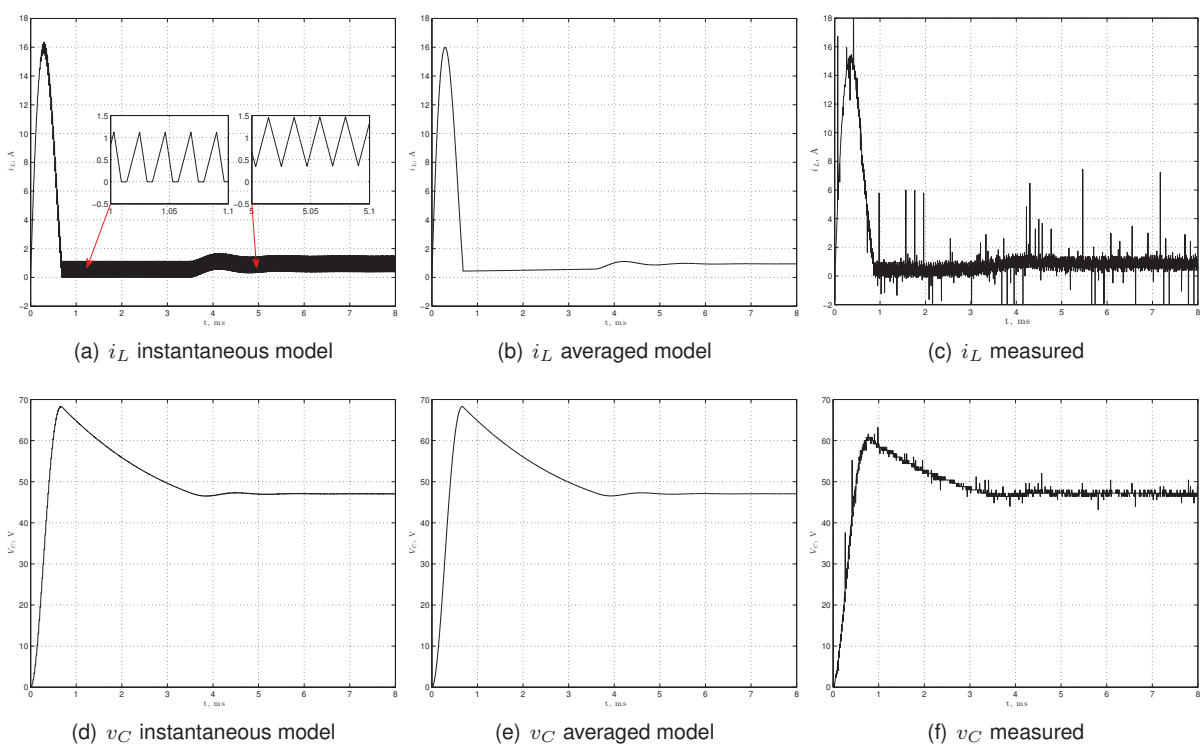


Fig. 5. Inductor current and capacitor voltage waveform comparisons.

Table 2. Numerical comparison between switching thresholds with ($R_L \neq 0$) and without ($R_L = 0$) inductor resistance.

Parameter	$R_L = 0$ (14) – (16)	$R_L \neq 0$ (18) – (21)
d_b	0.5	0.505924
I_{Lmb}	1.13743 A	1.13711 A
I_{Db}	0.284357 A	0.279840 A
I_{Lb}	0.568715 A	0.568662 A

$$I_{DRb} = -\frac{(\langle v_C(t) \rangle - V_s)}{R_L} (1 - d_{Rb}) + \frac{L}{R_L T} \left(I_{LmRb} + \frac{\langle v_C(t) \rangle - V_s}{R_L} \right) \left(1 - e^{-\frac{(1-d_{Rb})R_L T}{L}} \right), \quad (20)$$

$$(21) \quad I_{LRb} = \frac{V_s}{R_L} \left(d_{Rb} - \frac{L}{R_L T} \left(1 - e^{-\frac{R_L T}{L} d_{Rb}} \right) \right) + I_{DRb}.$$

Observe that if $T \ll \frac{L}{R_L}$ then the numerical differences resulting from using equations (14) – (16) when $R_L = 0$, versus (18) – (21) when $R_L \neq 0$ are minimal. This is illustrated in Table 2 where both sets of equations were used to calculate critical currents for a circuit composed of the elements from Table 1. As a consequence of these small differences, numerical values obtained for $R_L = 0$ were used in the averaged model simulations.

Figure 5 presents a comparison between simulated and measured waveforms of the inductor current $i_L(t)$ and the capacitor voltage $v_C(t)$. A step input voltage $V_s = 24V$ was used, the duty cycle was set to $d = 0.5$ and the initial conditions for the inductor current and the capacitor voltage were set to zero. All the test conditions are similar to those used in [12], and our results are in agreement with those, presented in that study.

Right after turning on the power the boost converter is operating in the CCM mode until about 0.75th millisecond. This is clearly demonstrated by the high, nonzero inductor current. This mode of operation is followed by the DCM mode until 3.5th millisecond. As presented in the inset of Fig. 5(a), where for a short interval in each cycle the inductor current decreases to zero. The DCM mode is followed by the CCM mode. The current oscillations are maintained, but the flow is uninterrupted.

Conclusions

The switched mode power supply model presented in this paper can be used to analyze the power supply operation in a variety of conditions. This model successfully predicts the operation characteristics in both continuous current (CCM) and discontinuous current (DCM) modes. We demonstrated that shapes of the open loop step response waveforms of the model and a real circuit are in agreement. However, in order to obtain exact numerical correspondences it is necessary to include non-ideal component models of passive and active elements. Furthermore, it appears that the averaged simulation model allows to increase the time discretization step leading to a reduction in the simulation time, however this leads to a decrease in the CCM/DCM switching instance accuracy.

One disadvantage of the proposed averaged model is the potential instability of the CCM/DCM mode switching. This instability, introduced by a feedback loop created by the first order transfer block, or a delay block in the inductor current, may cause the system to switch between modes with high frequency.

REFERENCES

- [1] V. M. Canalli, J. A. Cobos, J. A. Oliver, and J. Uceda. Behavioral large signal averaged model for dc/dc switching power converters. In *IEEE Power Electronics Specialists Conference*, volume 2, pages 1675–1681, Jun 1996.
- [2] P. Chrin and C. Bunlaksananusorn. Large-signal average modeling and simulation of dc-dc converters with simulink. In *Power Conversion Conference, PCC*, pages 27–32, April 2007.
- [3] R. W. Erickson, S. Cuk, and R. D. Middlebrook. Large-signal modeling and analysis of switching regulators. In *IEEE Power Electronics Specialists Conference*, pages 240–250, 1982.
- [4] R. Ghosh and G. Narayanan. A single-phase boost rectifier system for wide range of load variations. *IEEE Transactions on Power Electronics*, 22(2):470–479, March 2007.
- [5] F. Guinjoan, J. Calvente, A. Poveda, and L. Martinez. Large-signal modeling and simulation of switching dc-dc converters. *IEEE Transactions on Power Electronics*, 12(3):485–494, May 1997.
- [6] A. W. N. Husna, S. F. Siraj, and M. Z. Ab Muin. Modeling of dc-dc converter for solar energy system applications. In *IEEE Symposium on Computers Informatics, ISCI*, pages 125–129, March 2012.
- [7] W. Janke. Techniki opisu impulsowych przetwornic napięcia stałego. *Przegląd Elektrotechniczny*, 88(11b):5–10, November 2012.
- [8] W. Jiang, Y. Zhou, and J. Chen. Modeling and simulation of boost converter in ccm and dcm. In *International Conference on Power Electronics and Intelligent Transportation System, PTETIS*, volume 3, pages 288–291, Dec 2009.
- [9] M. Khan and A. K. Singh. Modeling and simulation of solar boost converter to supply power for cardiac pacemakers. In *IEEE International Symposium on Medical Measurements and Applications Proceedings, MeMeA*, pages 187–190, May 2013.
- [10] J. Lai and D. Chen. Design consideration for power factor correction boost converter operating at the boundary of continuous conduction mode and discontinuous conduction mode. In *Applied Power Electronics Conference and Exposition, APEC*, pages 267–273, Mar 1993.
- [11] D. Maksimovic and S. Cuk. A unified analysis of pwm converters in discontinuous modes. *IEEE Transactions on Power Electronics*, 6(3):476–490, Jul 1991.
- [12] D. Maksimovic, A. M. Stankovic, V. J. Thottuveilil, and G. C. Verghese. Modeling and simulation of power electronic converters. *Proceedings of the IEEE*, 89(6):898–912, Jun 2001.
- [13] S.R. Sanders and G. C. Verghese. Synthesis of averaged circuit models for switched power converters. In *IEEE International Symposium on Circuits and Systems*, volume 1, pages 679–683, May 1990.

Authors: Wojciech Błasinski, Ph. D., Institute of Automatic Control, Faculty of Electrical, Electronic, Computer and Control Engineering, Lodz University of Technology ul. Wólczańska 223, 90-924 Łódź, Poland, email: wojciech.blasinski@p.lodz.pl Henryk Błasinski, MSc., Department of Electrical Engineering, Stanford University, 450 Serra Mall, Stanford, CA, USA, email: h.blasinski@stanford.edu